

Cite this: *RSC Adv.*, 2017, 7, 38008

## Effect of metal–metal distance in Ni(II)-based metallo-supramolecular polymers: DNA binding and cytotoxicity†

Md. Delwar Hossain,<sup>‡a</sup> Utpal Rana,<sup>a</sup> Chanchal Chakraborty,<sup>a</sup> Jinghua Li,<sup>§a</sup> Reiko Nagano,<sup>b</sup> Takashi Minowa<sup>b</sup> and Masayoshi Higuchi<sup>\*,a</sup>

Received 19th May 2017

Accepted 25th July 2017

DOI: 10.1039/c7ra05644c

rsc.li/rsc-advances

Two Ni(II)-based metallo-supramolecular polymers (**polyNiL1** and **polyNiL2**) with different metal–metal distances were synthesized *via* (1 : 1) complexation between the Ni salts with bis(1,10-phenanthroline)s and their DNA binding properties and cytotoxicity were revealed. Short metal–metal distances (1.35 nm) in **polyNiL2** showed ~7 times stronger DNA binding properties and remarkably higher cytotoxicity to Hela-Fucci cells than long metal–metal distances (1.95 nm) in **polyNiL1**. Enhancement of Ni polymer-induced cell killing has been observed in a cell cycle study.

## Introduction

The construction of small molecules as anticancer drugs has been an intensive subject in the past few decades. Transition metal complexes as potential therapeutic agents have received more attention because the central metal atom can bound to a surrounding array of molecules or anions and the modified ligands can specifically recognize the sequence of a nucleic acid.<sup>1</sup> It is potentially useful to understand the binding of metal complexes to DNA, for designing the structure and conformation of metal complexes. The mode of recognition is a kind of reversible non-covalent binding primarily based upon intercalation, major or minor groove-binding, hydrogen bonding and electrostatic interactions, which are dependent on the spatial configuration and specific modification of small molecules.<sup>2</sup> As such, the development of new metal complex structures having high binding affinity with DNA is of increasing importance in drug design.<sup>2b</sup> In addition to the studies on the interaction between short strand planar complex and DNA, metal nanoparticles and polymer complexes have recently received more attention for application in antitumor targeted drug delivery.<sup>3</sup> Previously, we reported high binding affinity of terpyridine-based metallo-supramolecular polymers to DNA.<sup>4a,b</sup> These results indicate that the metallo-supramolecular polymers

become a new candidate of anticancer drugs, because such strong binding to DNAs should prevent multiplication of the cancer cells. Recently, we reported that, the right handed helical metallo-supramolecular polymer exhibited strong DNA binding properties to B-DNA and high cytotoxicity to cancer cell.<sup>4c</sup> Metallo-supramolecular polymer can bind to the DNA by strong electrostatic interaction and groove binding. Electrostatic interaction occurred between the positively charge metal center of polymer and negatively charge phosphate backbone of DNA. The phosphate–phosphate distance of B-DNA is 0.7 nm is well known.<sup>4d</sup> So, the metal–metal distance ~0.7 nm in metallo-supramolecular polymer should be a potential route for improving DNA binding properties, as a result of cytotoxicity. In order to enhance the possibility of metallo-supramolecular polymers as anticancer drugs, we planned to investigate the DNA binding activity of tetrahedral or square planar coordination geometry type metallo-supramolecular polymers with variation of the metal–metal distances. However, variety of *N*-hetero ligands such as terpyridines, bipyridines and porphyrins are well known for synthesis of metallo-supramolecular polymers but very few papers were reported with 1,10-phenanthroline based ligands.<sup>5</sup> Phenanthroline analogues formed coordinate metal complexes with variety of metal ions including Ni<sup>2+</sup>, Cu<sup>2+</sup>, Pt<sup>4+</sup> and have been shown numerous biological activities such as antitumour,<sup>6a</sup> anti-candida,<sup>6b</sup> anti-mycobacterial,<sup>6c</sup> antimicrobial,<sup>6d</sup> activities *etc.* Moreover, considerable attention has been focused on the use of phenanthroline complexes as intercalating agents of DNA<sup>1a</sup> and as artificial nucleases.<sup>7</sup> With the aim to generate biological activities of phenanthroline-based metallo-supramolecular polymers, herein we report the binding properties of Ni(II)-based polymers with ct-DNA and their cytotoxicity to cancer cells (Hela-Fucci). In addition, the variation of the metal–metal distances and their

<sup>a</sup>Electronic Functional Macromolecules Group, National Institute for Materials Science (NIMS), 1-1 Namiki, Tsukuba 305-0044, Japan. E-mail: HIGUCHI.Masayoshi@nims.go.jp; Fax: +81-29-860-4721; Tel: +81-29-860-4721

<sup>b</sup>Nanotechnology Innovation Station, NIMS, 1-2-1 Sengen, Tsukuba 305-0047, Japan

† Electronic supplementary information (ESI) available. See DOI: 10.1039/c7ra05644c

<sup>‡</sup> Present Address: Department of Chemistry, Faculty of Science, Jagannath University, Dhaka-1100, Bangladesh.

<sup>§</sup> Present Address: Laboratory of Soft Matter and Biological Physics, Institute of Physics, Chinese Academy of Sciences, Beijing 100190, China.



relationship to the binding affinity to DNA as well as anticancer activity to cancer cells also investigated.

## Experiment

### Materials

Calf-thymus (ct) DNA (TREVIGEN, 10 mg mL<sup>-1</sup>, 200–500 bp), was highly purified and qualified. Human cervical cancer (Hela) cells expressing the Fucci probes (Hela-Fucci) were purchased from RIKEN BRC, Japan. Cell Counting Kit-8 (CCK-8) was obtained from Dojindo Laboratories (Kumamoto, Japan). Fetal bovine serum (FBS) was obtained from Bioserum (Hiroshima, Japan). Dulbecco's Modified Eagle Medium (DMEM), Dulbecco's phosphate buffered saline (PBS), and trypsin-EDTA (0.05% trypsin, 0.53 mM EDTA-4Na) were obtained from Invitrogen (Carlsbad, CA, USA). Cell culture dishes were from BD Bioscience (San Jose, CA, USA). All reagents were the highest purity commercially available and, unless otherwise noted, were used as obtained without further purification.

### Instrumentation

UV-vis spectra were recorded at 30 °C using a Shimadzu UV-2550 UV-vis spectrophotometer. A Model 550 Microplate Reader (Bio-Rad Laboratories, Inc.) was used for cell viability test. Total Internal Reflection Fluorescence (TIRF), Leica microsystems were used for cell cycle study.

### Binding constant

The concentration of ct-DNA per nucleotide was calculated from its known extinction coefficient at 260 nm (6600 M<sup>-1</sup> cm<sup>-1</sup>, 200–500 base pairs) and the concentration of polymers were expressed in repeat units.<sup>8</sup> The binding constants of the polymers to ct-DNA were determined by absorption titration at 30 °C in 5% acetonitrile-aqueous solution. Dilution of the polymers at the end of each titration was negligible. The DNA binding constant,  $K_b$ , of the polymers were determined from fitting the changes in the absorption of the polymer as a function of ct DNA concentration using eqn (1).<sup>10</sup>

$$\frac{\varepsilon_a - \varepsilon_f}{\varepsilon_b - \varepsilon_f} = \frac{b - (b^2 - 2K_b^2 C_t [\text{DNA}]_t / s)^{1/2}}{2K_b C_t} \quad (1)$$

here  $b = 1 + K_b C_t + K_b [\text{DNA}]_t / 2s$ ,  $K_b$  is binding constant between polymer and DNA,  $C_t$  represents the total polymer concentration in repeat units,  $[\text{DNA}]_t$  is the DNA concentration per nucleotide, 's' is the size of the binding site per nucleotide and  $\varepsilon_a$ ,  $\varepsilon_f$ ,  $\varepsilon_b$  represent the apparent, free, and bound polymer molar extinction coefficients, respectively. The value of  $\varepsilon_b$  was determined from the plateau of DNA titration, at which point addition of DNA did not result in any further changes to the absorption spectrum.

### Cell viability

Human cervical cancer cell lines (Hela-Fucci) were maintained in DMEM medium supplemented with 5% fetal bovine serum (FBS), 100 IU mL<sup>-1</sup> of penicillin, 100 µg mL<sup>-1</sup> of streptomycin at

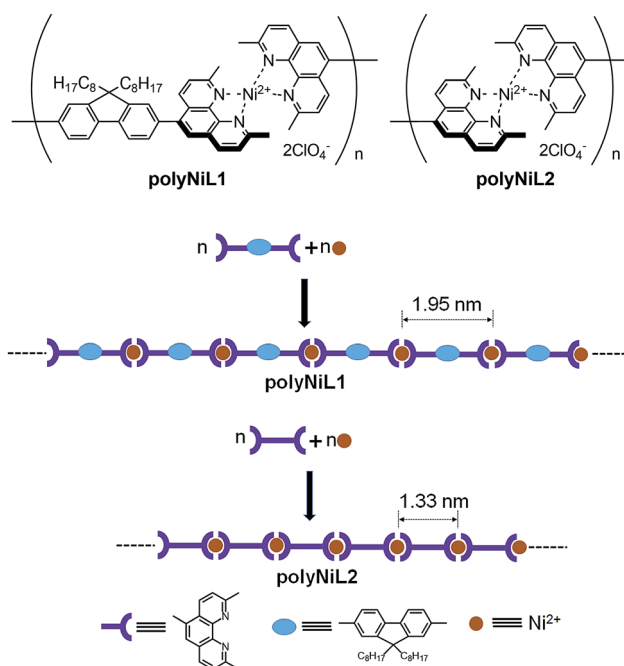
37 °C in a humidified incubator at 5% CO<sub>2</sub>. The adherent cultures were grown as monolayer and were passaged once in 3–4 days by exposure to 0.05% trypsin-EDTA. For cell viability assay, the Hela-Fucci cells were seeded in 96-well plates and cultured for 24 h. The medium was removed, and Ni polymers were added, which were prepared by medium including 5% acetonitrile and reached the final concentration 0, 5, 10, 15, 20, 25 µM respectively. The 5% acetonitrile was used as a control. After 24 h of incubation, 10 µL of CCK-8 solution was added to each well and check the cell viability. Further 24 h was incubated and check the cell viability. Cell viabilities were normalized to (OD450–OD620) for the untreated cells. Assays were performed in quadruplicate.

### Fluorescence imaging

Fluorescence images were taken using a fluorescence microscope (DMIL, Leica Microsystems, Germany). For time-lapse imaging, cells were held in an incubation chamber at 37 °C in a humidified atmosphere containing 5% CO<sub>2</sub> (Tokai Hit, Fujinomiya, Japan).

## Results and discussion

Bis(1,10-phenanthroline)s with different substituent **L1**–**L2** were synthesized according to our previous report.<sup>9a</sup> The **polyNiL1** and **polyNiL2** (Scheme 1) were prepared by 1 : 1 complexation equimolar **L1** or **L2** (in CH<sub>2</sub>Cl<sub>2</sub>), and Ni(ClO<sub>4</sub>)<sub>2</sub>·6H<sub>2</sub>O(CH<sub>3</sub>CN) under inert atmosphere.<sup>9b</sup> The reaction mixture was stirred 1 h at room temperature. The desired polymers were obtained as a pink solid (**PolyNiL1**: 92%; **polyNiL2**: 90%) and is highly soluble in acetonitrile. The molecular weight ( $M_w$ ) of **polyNiL1** and **polyNiL2** in acetonitrile were determined by



Scheme 1 Structures of the **polyNiL1** and **polyNiL2**.



a SEC-viscometry-RALLS method (size exclusion chromatography-viscometry-right-angle light scattering) using polyethylene oxide as a standard and to be  $1.24 \times 10^5$  Da and  $1.28 \times 10^5$  Da respectively.<sup>9</sup>

The coordination geometry of Ni(II) in polymers were justified by UV-vis spectrophotometric titration of Ni(II) ions and ligand **L1** (Fig. S1, ESI†) or **L2**.<sup>9b</sup> Interestingly, the spectrum changed during the addition of 0.0–1.0 equivalents of the Ni(II) salt to the ligand and then remained unaffected by the addition of more than 1.1 equivalents of the Ni(II) salt. The titration plots between the absorbance and the molar ratio of [the Ni salt]/[ligand] clearly showed the 1 : 1 complexation. These results indicated that Ni(II) bind 1 : 1 way and formed tetrahedral geometry during the formation of **polyNiL1** and **polyNiL2**.<sup>9a,b</sup>

The UV-vis spectra of **polyNiL1** and **polyNiL2** were recorded in 5% acetonitrile aqueous solution (concentration = 5 mM). The **polyNiL1** showed three absorption peaks at 230, 280 and 324 nm whereas **polyNiL2** showed two absorption peaks at 232 and 277 nm. The peaks at ~230 and ~280 nm for  $n \rightarrow \pi^*$  and  $\pi \rightarrow \pi^*$  transition of phenanthroline unit and 324 nm for  $\pi \rightarrow \pi^*$  transition of fluorene unit (Fig. S2, ESI†).<sup>9</sup>

The interaction between the polymers (**polyNiL1** and **polyNiL2**) and DNA was investigated by UV-vis spectral measurement (Fig. 1). Metallo-supramolecular polymers contains Ni(II) ions with bis(phenanthroline)s containing aromatic heterocycles, can be immensely powerful tools for probing nucleic acids. ct-DNA belongs to B-form DNA having wide major groove with moderate depths easily accessible to molecules. In the UV-vis titration with increasing concentrations of ct-DNA, all of Ni(II) polymers were found to exhibit noticeable hypochromism and bathochromic shift with several isosbestic points (Table 1). During the titration of ct-DNA to Ni(II) polymers, a hypochromic shift at 280–350 nm was observed due to electrostatic interaction between the polymer complexes and DNA (Fig. 1a and b). In UV-vis spectra, the hypochromicity along with bathochromic shifts indicate an electronic interaction between the polymers and ct-DNA. The spectral change was saturated at 1 : 1 molar ratio of [nucleotide of DNA]/[unit of polymer] (Fig. 1a and b insets). According to the fits of titration data (eqn (1)), the binding constants ( $K_b$ ) of **polyNiL1**, and **polyNiL2** were determined to be 2.77, and  $19.76 \times 10^6 \text{ M}^{-1}$  respectively by using the non-linear curve fitting (Table 1).<sup>10</sup> **PolyNiL1** with fluorene spacer has approximately seven times smaller binding constant than without spacer **polyNiL2**. The reason can be explained as the metal–metal distance in the polymer chains. The metal–metal distance for **polyNiL1** and **polyNiL2** was 1.95 and 1.33 nm respectively, which was calculated by simple Chem3D software. In contrast, the phosphate–phosphate distance of B-DNA are known to be approximately 0.7 nm. The charge of the Ni(II) atom in the polymer is +2, whereas the charge of the phosphate in DNA is –1. So, one Ni(II) center of polymer can interact with two phosphate groups of DNA. The metal–metal distance of polymers to phosphate–phosphate distance of DNA of **polyNiL1** and **polyNiL2** is approximately 2 and 3 respectively. So, strong electrostatic bonding between ct-DNA and **polyNiL2** occurred due to the close matching of the metal–metal distance of this polymer with phosphate–phosphate distance of B-DNA.

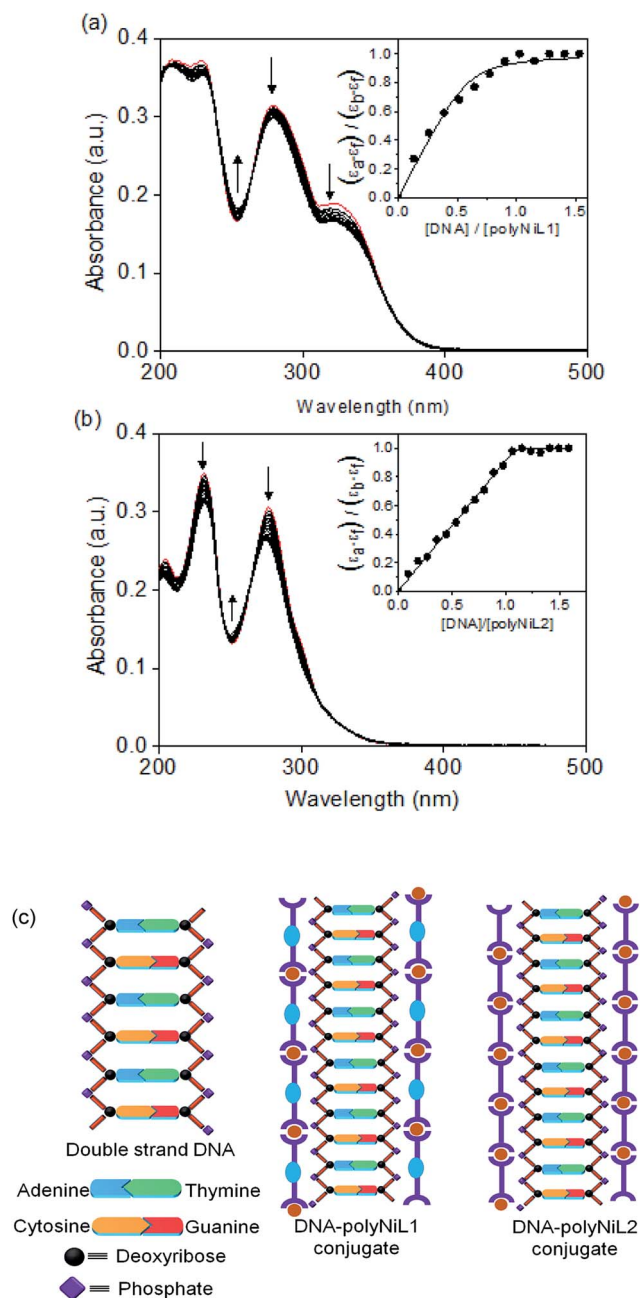


Fig. 1 UV-vis titration spectra of (a) **polyNiL1** (7  $\mu\text{M}$ : based on repeat unit), and (b) **polyNiL2** (7  $\mu\text{M}$ : based on repeat unit), in the absence and presence of increasing concentrations of ct-DNA (up to 7  $\mu\text{M}$ : per nucleotide of DNA) in aqueous solution including 5%  $\text{CH}_3\text{CN}$ . Red color for only polymers. The insets show titration plots at maximum absorbance for [nucleotide of DNA]/[unit of polymer] used to obtain the binding constant. (c) Estimation of conjugate structures of B-DNA and **polyNiL1** and **polyNiL2**.

Table 1 Calf thymus DNA binding of Ni(II) polymers

Polymer	Hypochromicity (%)	$K_b (\times 10^6 \text{ M}^{-1})$	$s$
<b>polyNiL1</b>	13	2.77	0.17
<b>polyNiL2</b>	14	19.76	0.49



Compared with the mono-metal complexes, the binding constants of the polymer complexes are larger than the mono-metal complexes.<sup>11</sup> Such a strong binding properties of the polymer complexes to ct-DNA will be caused by the collaborative effect on stabilization between the neighboring binding sites in the polymer complex. Therefore, very strong electrostatic interaction can be revealed between the Ni polymers and ct-DNA.

The structural changes of DNA in the presence of polymers were studied by circular dichroism (CD) titration and the results are shown in Fig. 2. The B-form of ct-DNA exhibited two positive bands at 277 and ~220 nm and a negative band at 248 nm (a black spectrum in Fig. 2a and b), implying the right-handed helical structure of DNA. When the polymer was added to the DNA solution, the spectrum was dramatically changed. The changes caused by **polyNiL2** were more significant than those by **polyNiL1**. Interestingly, with increasing the concentration of **polyNiL2**, the band at 277 nm in Fig. 2b was blue-shifted to 267 nm and almost vanished when the mass ratio of DNA/**polyNiL2** reached 1.0 : 0.2 (a green spectrum in Fig. 2b), indicating the original helical structure of DNA was collapsed. With the further addition of **polyNiL2** to the solution, a new band at 283 nm appeared in the negative region. This wavelength (283 nm) corresponds with that of an intense absorption (280 nm) in the UV-vis spectrum of **polyNiL2** (a black spectrum of Fig. S2, ESI†). This result indicates the helicity in **polyNiL2** was induced by DNA in the **polyNiL2**-DNA conjugates, probably because of the strong and favorable electrostatic interaction between the cationic **polyNiL2** and anionic DNA. It is considered that the polymer chains of **polyNiL2** take on a helical conformation along the DNA helicity.<sup>12a</sup> As for **polyNiL1**, with increasing the polymer concentration, the band at 277 nm in Fig. 2a became small but no new peaks appeared in the negative region. It suggests the electrostatic interaction with DNA is weaker than that of **polyNiL1**.

It is commonly considered that DNA is the major target of many anticancer agents.<sup>12b</sup> The aim of many studies is to establish new anticancer agents with greater selectivity to cancer cells. The cytotoxicity of the polymers (**polyNiL1**, **polyNiL2**) were studied using cell counting kit, CCK-8 (WST-8) assay with Hela-Fucci cell. The cytotoxicity of the polymers were measured as the percentage ratio of the absorbance of the treated Hela-Fucci cells to the untreated controls. Cell viability experiment showed 59.5% and 1% of viable cells with using **polyNiL1** (25  $\mu$ M) and **polyNiL2** (25  $\mu$ M) respectively (Fig. 3). The **polyNiL2** polymer without spacer largely decreased the cell

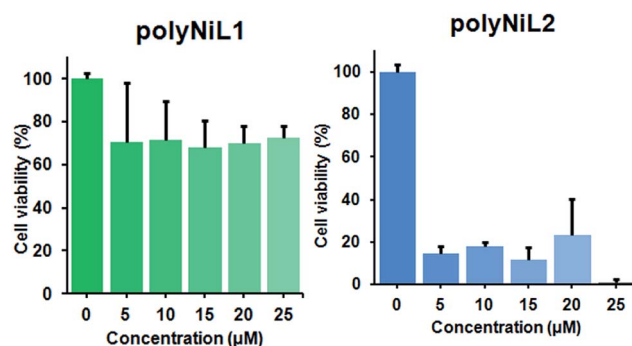


Fig. 3 Cytotoxicity of **polyNiL1** (0, 5, 10, 15, 20, 25  $\mu$ M) and **polyNiL2** (0, 5, 10, 15, 20, 25  $\mu$ M) in cell culture medium against Hela-Fucci cells.

viability in a dose-dependent manner than **polyNiL1** with fluorene spacer because the binding affinities of **polyNiL2** ( $K_b = 19.76 \times 10^6 \text{ M}^{-1}$ ) with ct-DNA is higher than **polyNiL1** ( $K_b = 2.77 \times 10^6 \text{ M}^{-1}$ ). It seems that the cytotoxicity of the polymers is largely dependent on the binding constant.

Cellstain-double staining kit is utilized for simultaneous fluorescence staining of viable and dead cells. This kit contains calcein-AM and propidium iodide (PI) solutions, which stain viable (green) and dead cells (red), respectively. After the cells were incubated for 24 h with 25  $\mu$ M of **PolyNiL1** or **polyNiL2** in 24 well plates, the cells were washed twice with sterile PBS, and 500  $\mu$ L of PBS containing calcein-AM (2  $\mu$ M) and PI (4  $\mu$ M) were added. Plates were incubated for 15 min before fluorescence imaging with a microscope. **PolyNiL2** (Fig. 4b) showed more number of dead cells (red fluorescence) than **polyNiL1** (Fig. 4a). Fluorescence microscopic analysis suggested that **PolyNiL2** has a greater potential to induce the death of Hela-Fucci cancer cells (Fig. 4) and indicates the higher cytotoxicity of **polyNiL2**.

Cell cycle study is the most important process for understanding the mechanism of DNA replication within a defined time period. Cell cycle occurs in four phases, G1(gap1)/S(synthesis)/G2(gap2)/M(mitosis).<sup>13</sup> A fluorescent probe that labels different phases of cell cycle like G1 phase nuclei in red and S/G2/M phase nuclei in green. Sakaue-Sawano *et al.* developed a cell-cycle visualization system called fluorescent ubiquitination-based cell-cycle indicator (Fucci), which takes advantage of the cell cycle-dependent ubiquitination of Cdt1 protein and geminin protein.<sup>13</sup> Fucci is a sophisticated technology for easy determination of G1 and S/G2/M phases of the cell cycle. Fucci-G1 red is a fusion protein of a fragment of

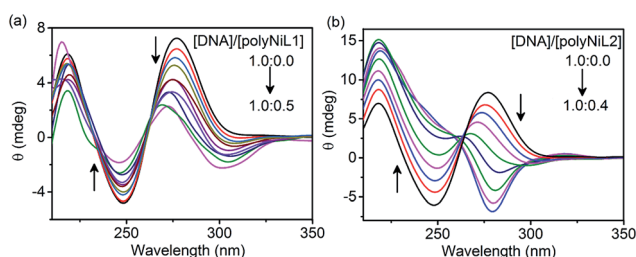


Fig. 2 CD spectra of (a) **polyNiL1** and (b) **polyNiL2**.

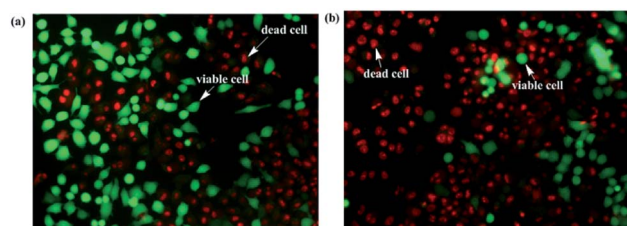


Fig. 4 Fluorescence images of Hela-Fucci cells treated with **polyNiL1** (a) and **polyNiL2** (b).



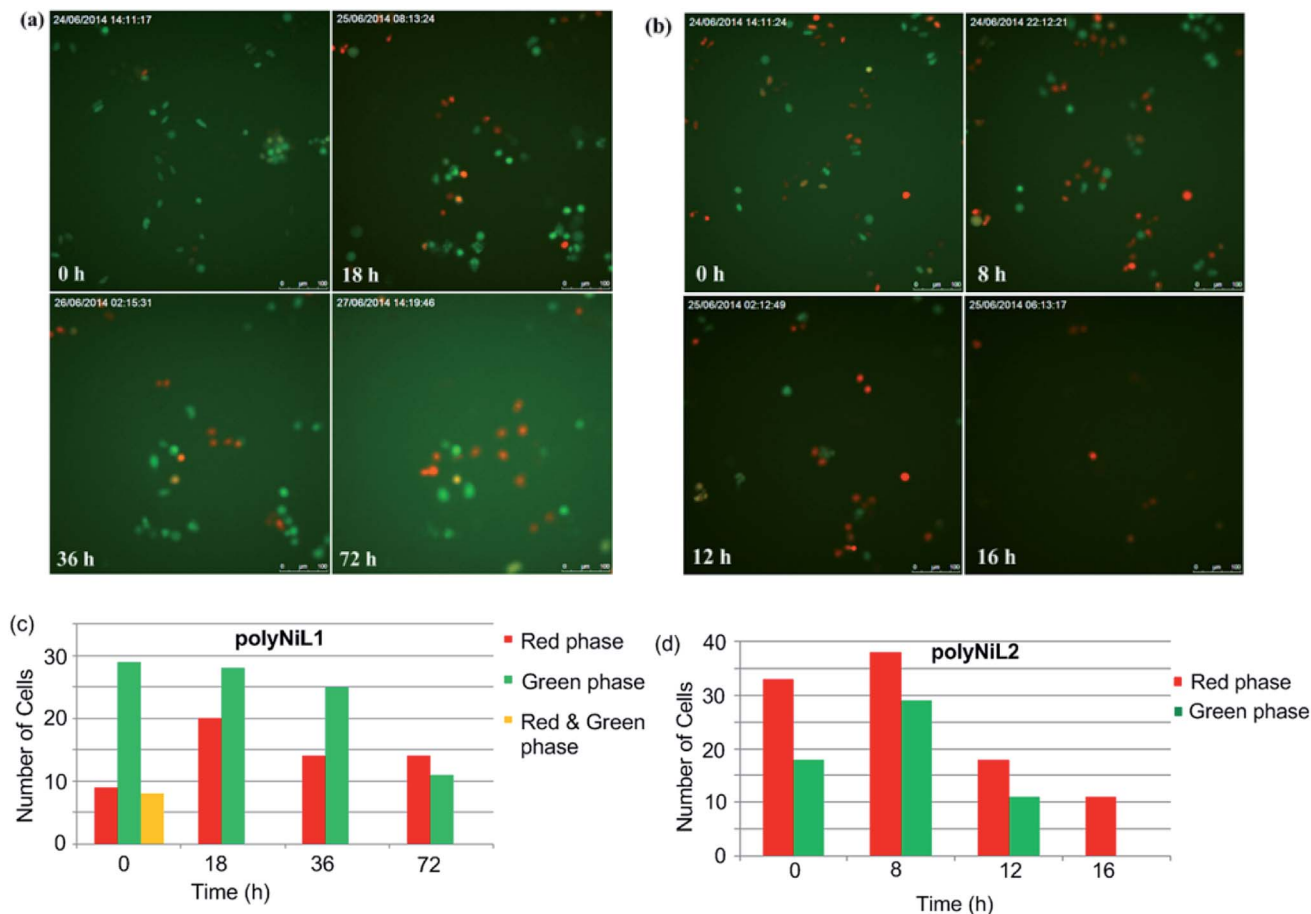


Fig. 5 Effects of Ni polymers in HeLa-Fucci cells using time-lapse imaging. (a) Representative images taken 0 to 72 h after treatment with polyNiL1. (b) 0 to 16 h after treatment with polyNiL2; red and green phases were changed with time by the treatment of (c) polyNiL1 and (d) polyNiL2.

human Cdt1 with the orange fluorescent, mKO2 (monomeric Kusabira-Orange2) that indicates the G1 phase, whereas Fucci-S/G2/M green is a fusion protein of a fragment of human geminin with the green fluorescent protein, mAG1 (monomeric Azami-Green1) that visualize S/G2/M phase.<sup>13c</sup> In this system, G1 and S/G2/M cells emit red and green fluorescence by TIRF microscope, respectively. In our experiment, we added Ni polymer solution in HeLa-Fucci cells in DMEM then held in TIRF microscope. In Fig. 5a and c, we have shown that G1 (red phase) and S/G2/M (green phase) HeLa-Fucci cells gradually decreased during 0 h to 72 h treatment with polyNiL1 (25  $\mu$ M). In Fig. 5b and d, G1 and S/G2/M cells drastically decreased during 0 h to 16 h with polyNiL2 (25  $\mu$ M) and finally only G1 cells remained. This result indicated that G1 phase is arrested with the treatment of polyNiL2 and predicted to enhance cell killing. Thus, we concluded that the polyNiL2 showed very strong cytotoxicity than polyNiL1.

## Conclusions

In an effort to select the new candidates for anti-cancer drugs, we used our synthesized polymers (polyNiL1, and polyNiL2) to do the DNA binding experiments. The very strong electrostatic

interaction was confirmed between the polymers and ct-DNA by UV-vis experiment. The polyNiL2 exhibited higher binding constants than polyNiL1 to ct-DNA. Cell viability experiment showed 59.5% and 1% of viable cell for polyNiL1 and polyNiL2 to cancer cells (HeLa-Fucci) respectively. Cell cycle studies showed living cancer cell dead rapidly with the treatment with polyNiL2.

## Acknowledgements

The authors would like to acknowledge JST CREST Grant Number JPMJCR1533, Japan for financial support.

## References

- (a) K. E. Erkkila, D. T. Odom and J. K. Barton, *Chem. Rev.*, 1999, **99**, 2777; (b) S. N. Georgiades, N. H. Abd Karim, K. Suntharalingam and R. Vilar, *Angew. Chem., Int. Ed.*, 2010, **49**, 4020; (c) J. K. Barton, E. D. Olmon and P. A. Sontz, *Coord. Chem. Rev.*, 2011, **255**, 619.
- (a) B. C. Bales, T. Kodama, Y. N. Weledji, M. Pitie, B. Meunier and M. M. Greenberg, *Nucleic Acids Res.*, 2005, **33**, 5371; (b)



- J. Liu, H. Zhang, C. Chen, H. Deng, T. Lu and L. Ji, *Dalton Trans.*, 2003, **115**, 114.
- 3 (a) Y. Matsumura and H. Maeda, *Cancer Res.*, 1986, **46**, 6387; (b) C. H. J. Choi, C. A. Alabi, P. Webster and M. E. Davis, *Proc. Natl. Acad. Sci. U. S. A.*, 2010, **107**, 1235.
- 4 (a) J. Li, Z. Futera, H. F. Li, Y. Tateyama and M. Higuchi, *Phys. Chem. Chem. Phys.*, 2011, **13**, 4839; (b) J. Li, T. Murakami and M. Higuchi, *J. Inorg. Organomet. Polym.*, 2013, **23**, 119; (c) U. Rana, C. Chakraborty, R. K. Pandey, M. D. Hossain, R. Nagano, H. Morita, S. Hattori, T. Minowa and M. Higuchi, *Bioconjugate Chem.*, 2016, **27**, 2307; (d) R. J. Epstein, *Human Molecular Biology: An Introduction to the Molecular Basis of Health and Disease*, Cambridge University Press, Cambridge, 2003.
- 5 (a) A. T. Daniher and J. K. Bashkin, *Chem. Commun.*, 1998, 1077; (b) P. J. Carter, C.-C. Cheng and H. H. Thorp, *J. Am. Chem. Soc.*, 1998, **120**, 632; (c) R. J. Mortimer, A. L. Dyer and J. R. Reynolds, *Displays*, 2006, **27**, 2; (d) D. G. Kurth and M. Higuchi, *Soft Matter*, 2006, **2**, 915; (e) M. Higuchi and D. G. Kurth, *Chem. Rec.*, 2007, **7**, 203; (f) F. S. Han, M. Higuchi and D. G. Kurth, *Adv. Mater.*, 2007, **19**, 3928; (g) F. S. Han, M. Higuchi and D. G. Kurth, *J. Am. Chem. Soc.*, 2008, **130**, 2074; (h) A. Bandyopadhyay, S. Sahu and M. Higuchi, *J. Am. Chem. Soc.*, 2011, **133**, 1168; (i) G. R. Whittell, M. D. Hager, U. S. Schubert and I. Manners, *Nat. Mater.*, 2010, **10**, 176; (j) R. I. Wojtecki, M. A. Meador and S. J. Rowan, *Nat. Mater.*, 2010, **10**, 14; (k) M. Burnworth, L. Tangl, J. R. Kumpferl, A. J. Duncan, F. L. Beyer, G. L. Fiore, S. J. Rowan and C. Weder, *Nature*, 2011, **472**, 334; (l) U. Velten, B. Lahn and M. Rehahn, *Macromol. Chem. Phys.*, 1997, **198**, 2789; (m) U. Velten and M. Rehahn, *Chem. Commun.*, 1996, 2639; (n) S. Bernhard, K. Takada, D. Jenkins and H. D. Abruna, *Inorg. Chem.*, 2002, **41**, 765; (o) S. Bernhard, J. I. Goldsmith, K. Takada and H. D. Abruna, *Inorg. Chem.*, 2003, **42**, 4389; (p) U. Velten and M. Rehahn, *Macromol. Chem. Phys.*, 1998, **199**, 127; (q) P. L. Vidal, B. Divisia-Blohorn, G. Bidan, J. L. Hazemann, J. M. Kern and J. P. Sauvage, *Chem.-Eur. J.*, 2000, **6**, 1663; (r) J. P. Sauvage, *Acc. Chem. Res.*, 1998, **31**, 611.
- 6 (a) J. D. Ranford and P. J. Sadler, *Dalton Trans.*, 1993, 3393; (b) G. Majella, S. Vivienne, M. Malachy, D. Michael and M. Vickie, *Polyhedron*, 1999, **18**, 2931; (c) D. K. Saha, U. Sandbhor, K. Shirisha, S. Padhye, D. Deobagkar, C. E. Ansond and A. K. Powell, *Bioorg. Med. Chem. Lett.*, 2004, **14**, 3027; (d) M. A. Zoroddu, S. Zanetti, R. Pogni and R. Basosi, *J. Inorg. Biochem.*, 1996, **63**, 291.
- 7 (a) D. S. Sigman, *Biochem.*, 1990, **29**, 9097; (b) D. S. Sigman, A. Mazumder and D. M. Perrin, *Chem. Rev.*, 1993, **93**, 2295; (c) W. K. Pogozelski and T. D. Tullius, *Chem. Rev.*, 1998, 1089.
- 8 R. E. Reichmann, S. A. Rice, C. A. Thomas and P. Doty, *J. Am. Chem. Soc.*, 1954, **76**, 3047.
- 9 (a) M. D. Hossain and M. Higuchi, *Synthesis*, 2013, **45**, 753; (b) R. K. Pandey, M. D. Hossain, S. Moriyama and M. Higuchi, *J. Mater. Chem. A*, 2013, **1**, 9016; (c) M. K. Bera, C. Chakraborty and S. Malik, *New J. Chem.*, 2015, **39**, 9207–9214.
- 10 (a) W. A. Kalsbeck and H. H. Thorp, *J. Am. Chem. Soc.*, 1993, **115**, 7146; (b) D. A. Lutterman, A. Chouai, Y. Liu, Y.-J. Sun, C. D. Stewart, K. R. Dunbar and C. Turro, *J. Am. Chem. Soc.*, 2008, **130**, 1163; (c) Y. Liu, R. Hammitt, D. A. Lutterman, R. P. Thummel and C. Turro, *Inorg. Chem.*, 2007, **46**, 6011; (d) V. Uma, M. Elango and B. U. Nair, *Eur. J. Inorg. Chem.*, 2007, 3484; (e) M. Marigppan and B. G. Maiya, *Eur. J. Inorg. Chem.*, 2005, 2164.
- 11 (a) S. Ramakrishnan and M. Palaniandavar, *J. Chem. Sci.*, 2005, **117**, 179; (b) H. Gopinathan, A. E. Poornanandhan and M. N. Arumugham, *International Journal of Inorganic and Bioinorganic Chemistry*, 2012, **2**, 42; (c) S. Arounagiri, D. Easwaramoorthy, A. Ashokkumar, A. Dattagupta and B. G. Maiya, *Proc. - Indian Acad. Sci., Chem. Sci.*, 2000, **112**, 1.
- 12 (a) H. Qiu, J. B. Gilroya and I. Manners, *Chem. Commun.*, 2013, **49**, 42–44; (b) F. Gao, H. Chao, F. Zhou, Y. X. Yuan, B. Peng and L. N. Ji, *J. Inorg. Biochem.*, 2006, **100**, 1487.
- 13 (a) N. Zielke and B. A. Edgar, *Wiley Interdiscip. Rev.: Dev. Biol.*, 2015, **4**, 469; (b) A. Sakaue-Sawano, H. Kurokawa, T. Morimura, *et al.*, *Cell*, 2008, **132**, 487; (c) S. Karasawa, T. Araki, T. Nagai, H. Mizuno and A. Miyawaki, *Biochem. J.*, 2004, **381**, 307.

